Chemistry and Physics of Lipids 220 (2019) 49–56

Contents lists available at ScienceDirect

Chemistry and Physics of Lipids

journal homepage: www.elsevier.com/locate/chemphyslip

Charged phospholipid effects on AAPH oxidation assay as determined using liposomes

Kervin O. Evans[a,*], David L. Compton[a], Sanghoon Kim[b], Michael Appell[c]

[a] Renewable Products Technology Research Unit, United States
[b] Plant Polymer Research Unit, USDA, United States
[c] Mycotoxin Prevention and Applied Microbiology Research Unit, National Center for Agricultural Utilization Research, 1815 N. University Street, Peoria, IL, 61604, United States

ARTICLE INFO

Keywords:
Charged phospholipids
AAPH
Liposomes
Rate-limiting
Oxidation
Kinetics

ABSTRACT

The capacity of molecules to inhibit oxidation is widely tested using liposomes as host matrices of the antioxidant molecule of interest. Spectroscopic assays are readily used for this purpose, specifically assays using 2,2′-azobis(2-methylpropionamidine) dihydrochloride (AAPH). In this work the effect that charged lipids have on an AAPH antioxidation assay using 4,4-difluoro-5-(4-phenyl-1,3-butadienyl)-4-bora-3a,4a-diaza-s-indacene-3-undecanoic acid (C_{11}-BODIPY® 581/591) as the reporter molecule was investigated. We measured the diameter, zeta potential and spectroscopic rate of decay and area-under-the-curve (AUC) associated with liposomes containing C_{11}-BODIPY® 581/591 at varying molar percentages (0–10 mol%) of charged (cationic or anionic) lipids and compared the results. We showed that although increasing amounts of cationic or anionic lipids did change the diameter of the liposomes, size had little to no effect on the area-under-the-curve or decay rate of fluorescence. Increased (more positive) or decreased (more negative) zeta potentials did, on the other hand, affect the spectroscopic decay rates and area-under-the-curve. The results demonstrate the importance of considering the presence of charged lipids in the AAPH antioxidation assay.

1. Introduction

Oxidation causes degradation of lipids and is a major cause of rancidity in fats and oils worldwide, especially in the food industry. Several methods, such as encapsulating anitoxidants within liposomes (Balanč et al., 2015) and enhancing oils with antioxidant properties (Laszlo et al., 2013; Evans and Compton, 2017; Compton et al., 2017) for incorporation within liposomes, have been employed to combat the loss of quality in oils and fats. It, therefore, is important to measure antioxidation capacity of bioactives within liposomes.

Typically, antioxidation measurements for bioactives within liposome systems involve the use of a radical initiator like 2,2′-azobis(2-methylpropionamidine) dihydrochloride (AAPH) (Laszlo et al., 2013; Tikekar and Nitin, 2011; Mosca et al., 2011; An et al., 2011; Laszlo et al., 2010). AAPH is an aqueous-soluble molecule that thermally breaks down into two peroxy radicals capable of oxidizing targeted species (Zhang et al., 2006).

Liposomes are versatile and simple versions of cells that, typically, contain primarily lipids. The fact that most lipids are miscible make liposomes highly versatile and readily tunable for various environments. Past studies have demonstrated that the phase state of liposomes can attenuate the oxidation process (Tikekar and Nitin, 2011; Bricarello et al., 2012), and have also demonstrated that the charge state of lipid matrices like emulsions and micelles can affect the oxidation of lipids (Mei et al., 1999, 1998). This work was conducted to investigate how the charged state of liposomes affects the oxidation process within liposomes. This study utilized anionic and cationic phospholipid species incorporated within phosphatidylcholine-based liposomes.

2. Materials and methods

1,2-Dioleoyl-*sn*-glycero-3-phosphocholine (DOPC), 1,2-dimyristoyl-*sn*-glycero-3-phosphocholine (DMPC), 1,2-dipalmitoyl-*sn*-glycero-3-phosphocholine (DPPC), 1,2-dioleoyl-sn-glycero-3-phospho-(1′-*rac*-glycerol) (DOPG), 1,2-dimyristoyl-*sn*-glycero-3-phospho-(1′-*rac*-glycerol)] (DMPG), 1,2-dipalmitoyl-*sn*-glycero-3-phospho-(1′-*rac*-glycerol) (DPPG), 1,2-dioleoyl- *sn*-glycero-3-ethylphosphocholine (DOEPC), 1,2-dimyristoyl-*sn*-glycero-3-ethylphosphocholine (DMEPC), and 1,2-dipalmitoyl-*sn*-glycero-3-ethylphosphocholine (DPEPC) were purchased from Avanti Polar

* Corresponding author.
E-mail address: Kervin.Evans@ars.usda.gov (K.O. Evans).

https://doi.org/10.1016/j.chemphyslip.2019.02.004
Received 26 September 2018; Received in revised form 21 December 2018; Accepted 19 February 2019
Available online 21 February 2019
0009-3084/ Published by Elsevier B.V.

Lipids, Inc. (Alabaster, AL). 4,4-difluoro-5-(4-phenyl-1,3-butadienyl)-4-bora-3a,4a-diaza-s-indacene-3-undecan oic acid (C_{11}-BODIPY® 581/591) was purchased from ThermoFisher Scientific. 2,2′-azobis(2-methylpropionamidine) dihydrochloride (AAPH) and 2-amino-2-(hydroxymethyl)-1,3-propanediol hydrochloride (TRIS − HCl) were purchased from Sigma-Aldrich (Waltham, MA). Sodium chloride and calcium chloride were purchased from Fisher Scientific (St. Louis, MO).

3. Experimental procedures

3.1. Liposome preparation

Liposomes were created via the hydration method as previously described (Evans, 2006). Lipids in chloroform or 2:1 chloroform:methanol mix were dried under a gentle stream of argon and subsequently dried under a vacuum for 3 h. Lipids were hydrated in the appropriate buffers and vigorously mixed for at least 30 min. Hydrated lipids were subsequently put through five cycles of freezing and thawing using dry ice in ethanol and a 60 °C water bath, respectively. Hydrated lipids were finally extruded 11-times through two 100-nm filters using a LiposoFast hand-held extruder (AVESTIN, Inc., Ottawa, Canada). All manipulations were done above the phase transition temperature of the respective phospholipid explored.

3.2. Particle size, zeta potential

Dynamic light scattering (DLS) experiments were carried out using a Particle Size Analyzer (Model NanoBrook Omni, Brookhaven Instruments Corporation, Holtsville, NY, USA) equipped with a 658 nm diode laser and an avalanche photodiode detector. All measurements were done at 90° detection angle at 23.0 °C. For each sample, ten measurements were conducted and each run lasted 20 s. These data were averaged to obtain the size of particles. All measurements were processed using the software supplied by the manufacturer (9kpsdw, v.5.31), which provided the mean hydrodynamic diameter via a multimodal analysis. The electrophoretic mobilites, and hence the calculated zeta potentials, were determined by electrophoresis and phase analysis light-scattering (PALS) using a Zeta-PALS function of the aforementioned Particle Size Analyzer. Ten measurements were carried out for each sample at 23.0 °C. All the data were taken and processed using the software supplied by the manufacturer (PALS Zeta Potential Analyzer, version 5.73). The average of 10 measurements and the standard deviation are reported.

3.3. AAPH antioxidation assay

The antioxidation assay used was based on the fact that each molecule of radical initiator AAPH broke down into two radicals that oxidize the hydrophobic reporter molecule C_{11}-Bodipy 581/591 (Zhang et al., 2006). The antioxidation assay in this study was modified from previous work (Laszlo et al., 2010). Accordingly, lipids were combined to a total stock concentration of 3.75 mM. C_{11}-Bodipy 581/591, stored in ethanol, was added to give a stock concentration of 3.6 μM. The lipid mixture was gently mixed and dried under a gentle argon stream to a thin film. Lipids were further dried for 3 h using a condenser speed vacuum unit and stored under argon at -20 °C until needed. Lipids were hydrated in buffer (20 mM Tris − HCl, pH 7.4) and mixed for 30 min prior to going through five cycles of freeze/thaw (dry ice in ethanol/60 °C waterbath). We created liposomes by extruding the hydrated lipids 11-times through double-stacked filters with 100-nm pores using a LiposoFast hand-held extruder (Avestin, Inc., Ottowa, ON, Canada). Liposomes were stored at room temperature prior to use. We diluted the lipids and C_{11}-Bodipy 581/591 to a final concentration of 0.25 mM and 0.24 μM, respectively, in the cuvette. Liposomes were allowed to equilibrate to 37 °C just prior to adding enough AAPH for a final concentration of 4 mM. Triplicate to sextuplicate measurements were conducted; the average for each series is reported here.

4. Results and discussion

4.1. Effect of anionic lipids on AAPH antioxidation assay

The effect of anionic lipids on oxidation rates of the reporter molecule Bodipy™ 581/591 was determined in DOPC liposomes containing DOPG from 0 to 10 mol%. We chose DOPC and DOPG because each lipid had the same acyl chain length and same degree of acyl chain saturation (18:1) which resulted in all lipids having nearly the same phase transition temperatures (-20 °C and − 18 °C for DOPC and DOPG, respectively). This ensures that all lipids are in the same phase state at the experimental temperature (37 °C), and there were negligible effects due to lipid phase[10]. This also made negligible, or eliminated, any effects due to varying acyl chain lengths. Fig. 1 displays the results of the AAPH antioxidation assay as a function of increased DOPG within the liposomes. The data show that generated AAPH radicals that oxidized the reporter Bodipy molecule caused a loss of fluorescence signal more rapidly as DOPG concentration increased (Fig. 1a) within liposomes. This loss in the fluorescence signal due to increasing DOPG concentration also correlated to declining area-under-the-curve (AUC) values and increasing decay rates (Fig. 1b). Fig. 1b shows that the AUC values decreased linearly with respect to DOPG concentration. All decay curves fit well to a single-exponential decay ($A_o e^{-rt}$ where A_o is the initial concentration, r is the decay rate constant and t is time in min), which suggests that C_{11}-Bodipy 581/591 fluorescence loss is well described by a first-order reaction. Analysis of the curves' decay rates (Fig. 1b) showed that they were of the order (from slowest to fastest): 100:0 > 99:1 > 98:2 > 95:5 > 90:10, DOPC:DOPG mol% ratios. Analysis also showed that the decay rates increased nearly linearly up to 5 mol% DOPG. All of this suggests that lipids oxidize faster when negatively charged lipids are present; this agreed well with previous studies that showed lipid oxidation occurred much faster

when positively charged ions (Fe^{3+} and Cu^{2+}) were in the presence of both negatively charged emulsions (Mei et al., 1998) and in systems composed of negatively charged fatty acid micelles (Yoshida and Niki, 1992).

Comparison was also conducted for liposomes containing phospholipids that have saturated acyl chains but were in a fluid state at 37 °C. DMPC and DMPG both have a phase transition temperature of 23 °C, exist in a complete fluid state at experimental temperature (data not shown), and were zwitterionic and anionic, respectively, under the experimental conditions. Fig. 2a shows that the fluorescence signal was lost more rapidly as the concentration of DMPG was increased within DMPC liposomes, similar to experiments for DOPC:DOPG mixtures; Fig. 2b shows corresponding decreasing AUC values and increasing decay rates with respect to increasing DMPG concentrations, same as was shown for DOPC and DOPG mixtures. Analysis also shows that the AUC decreased and fluorescence decay rates increased, both exponentially in relationship to DMPG concentration within DMPC liposomes. The fact that the AUC values and decay rates for DOPC:DOPG mixtures are, respectively, at least three-times smaller and three-times faster, respectively, than those for DMPC:DMPG mixtures suggests that the presence of saturatured lipids, even in a fluid state, can impede lipid oxidation. This agrees well with findings of Bricarello et al, 2012 (Bricarello et al., 2012) who demonstrated that the physical state of lipids hindered lipid oxidation. Evidence presented here also suggests that the physical state of the lipids also to some extent counteracts the ability of negatively charged lipids to speed up oxidation.

Comparison of liposomes still in the gel state under the current conditions was done using a mixture of DPPC (zwitterionic) and DPPG

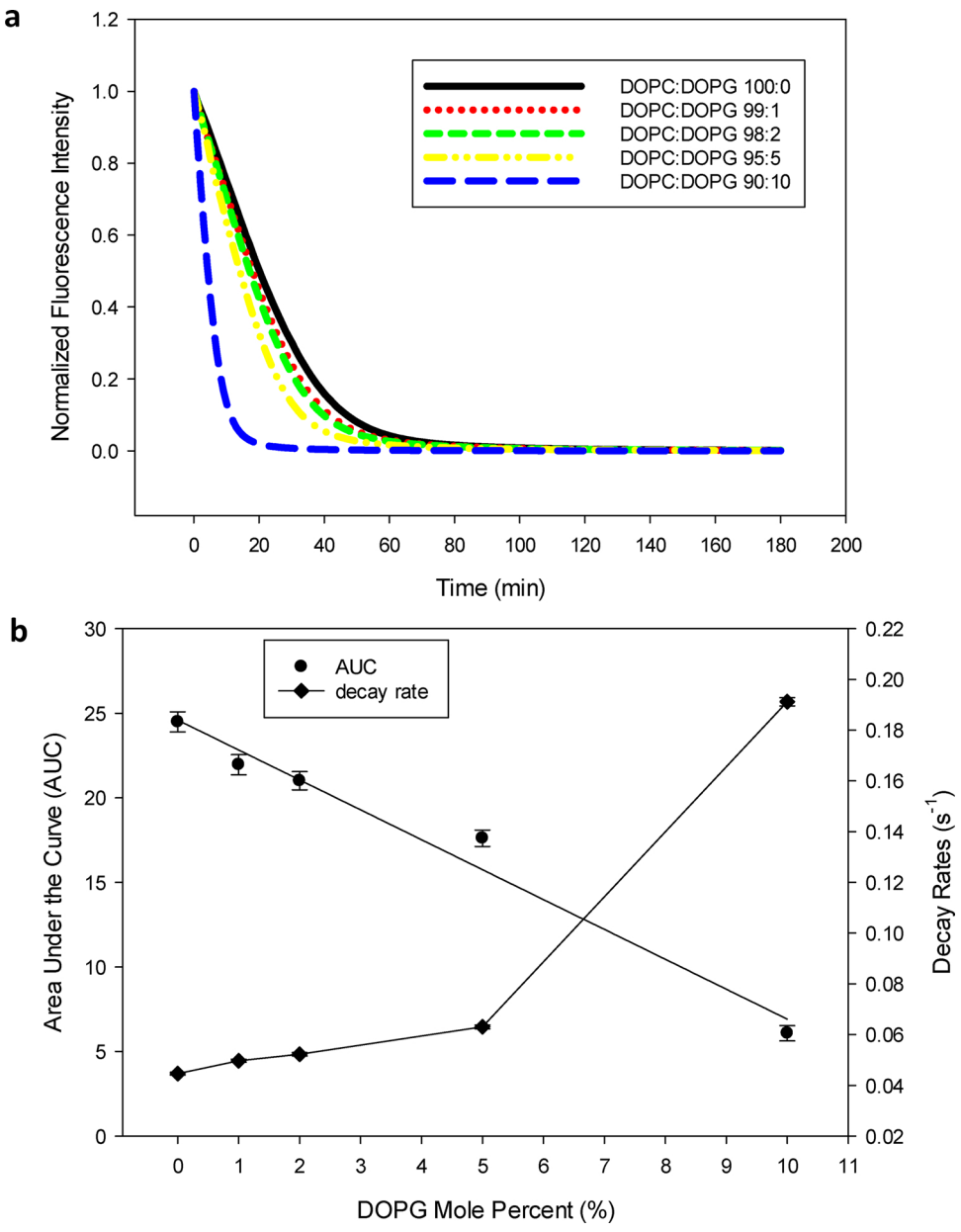

Fig. 1. a **The kinetics of the normalized fluorescence intensity for Bodipy 581/591 as a function of DOPG presence in DOPC liposomes.** Time course for the oxidation of Bodipy 581/591 in DOPC liposome with varying concentrations of DOPG at either 0, 1, 2, 5 or 10 mol percent; oxidation was due to the thermal degradation of AAPH at 37 °C. Data represents the average of 3–6 experiments. b **Area-under-the curve and decay rate plot as a function of DOPG.** Values for the area-under-the-curve (left) and decay rates for the normalized fluorescence signal of Bodipy 581/591 plotted as a function of DOPG mole percent presence in DOPC liposomes. The error bars shown are the calculated standard deviations.

(anionic) lipids where both have a phase transition temperature of 41 °C. Fig. 3a shows the results of the AAPH antioxidation assays as a function of DPPG concentration. Similar to the two previous measurements using phosphatidylglycerol lipids, the loss of fluorescence was faster as more anionic lipid (DPPG, in this case) was present within the liposomes. It was also noticeable that AUC values decreased exponentially and decay rates increased nearly exponentially as a function of DPPG concentration (Fig. 3b).

4.2. Effect of cationic lipids on AAPH

Comparison of the effects of cationic (positively) charged lipids (ethylphosphatidylcholine - EPC) was also investigated. Lipids of comparable saturation and acyl chain length (i.e. DOPC:DOEPC, DMPC:DMEPC, and DPPC:DPEPC) were again matched together and employed to minimize or eliminate any effects that could be due to varying lipid phases throughout the membrane. DOPC liposomes containing DOEPC exhibited increased ability to retain the fluorescence signal of C_{11}-Bodipy 581/591 as the amount of DOEPC present in the lipid membrane went from 0 to 10 mol%, as evidenced in Fig. 4a.

The increased retention of fluorescence signal also correlated into the AUC values and decay rates, respectively, increasing and decreasing linearly as a function of DOEPC concentration (supplemental Fig. 1). Liposomes containing DMPC with increasing amounts of DMEPC, on the other hand, exhibited little to no change in fluorescence signal from 0 to 2 mol% DMEPC, but did show an increasing fluorescence signal from 2- mol% DMEPC to 10 mol% DMEPC. Analysis of the AUC values for DMEPC-containing liposomes reveals a similar trend in that AUC values changed little as well over DMEPC concentration of 0 to 2 mol% and but are best described as sigmoidal in nature. The decay rates for liposomes with DMEPC also stayed relatively the same from 0 to 2 mol % DMEPC, but decreased beyond 2-mole percent DMEPC presence (supplemental Fig. 2). DPEPC-containing liposomes exhibited a similar trend to DMEPC-containing liposomes where there was little to no change in fluorescence intensity for 0, 1 and 2 mol%DPEPC, but greater retention of fluorescence signal for DPPC liposomes containing 2, 5, and

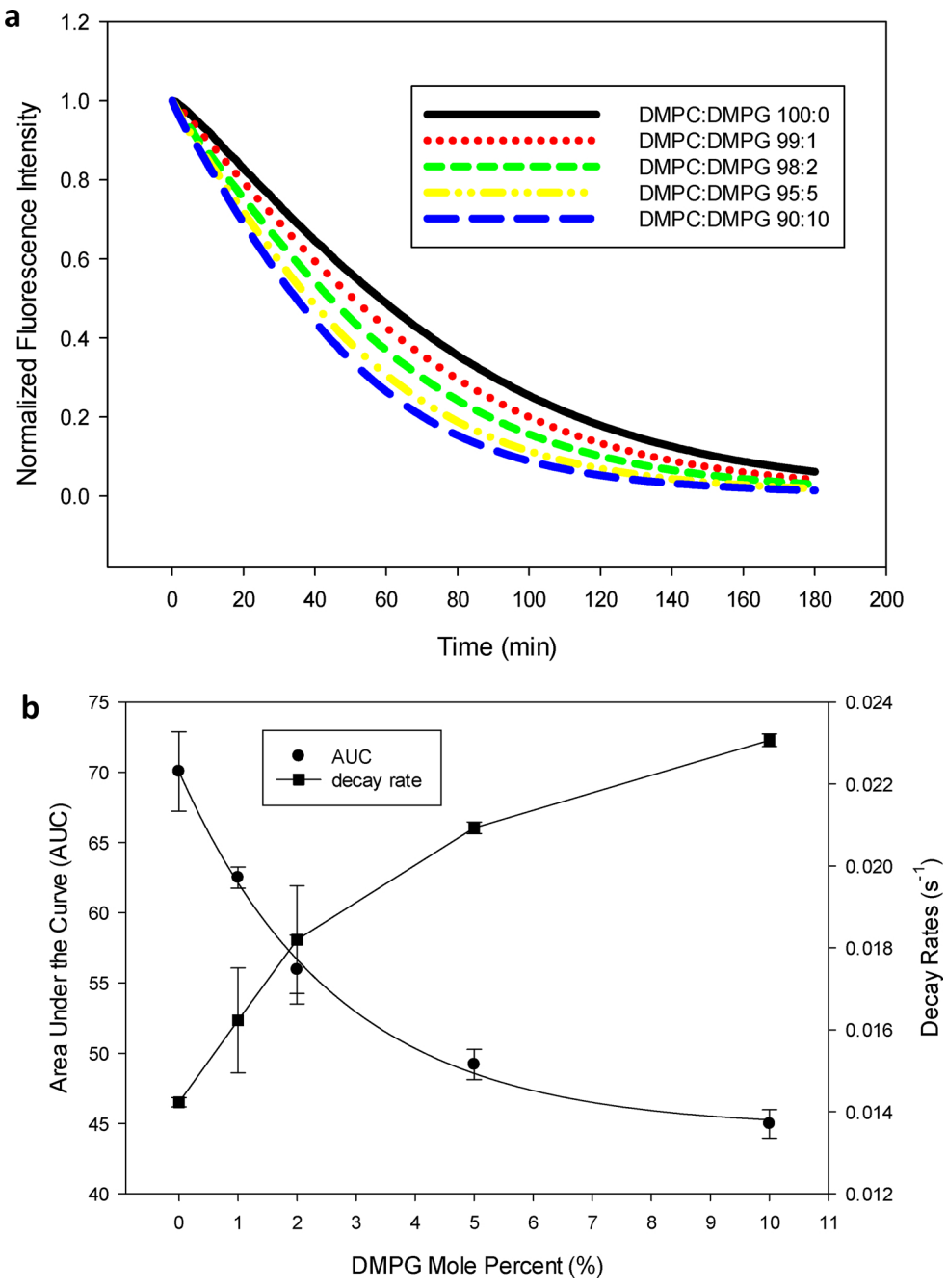

Fig. 2. a **The kinetics of the normalized fluorescence intensity for Bodipy 581/591 is shown as a function of DMPG presence in DMPC liposomes.** Time course for the oxidation of Bodipy 581/591 in DMPC liposome with varying concentrations of DMPG at either 0, 1, 2, 5 or 10 mol percent; oxidation was due to the thermal degradation of AAPH at 37 °C. The data displayed is the average of 3–6 experiments. b **Area-under-the-curve and decay rates as a function of DMPG.** Plot of the area-under-the-curve (left) and decay rates for the normalized fluorescence of Bodipy 581/591 as a function of DMPG concentration in DMPC liposomes. The error bars shown are the calculated standard deviations.

10 mol%DPEPC (Fig. 4c). This, too, translated into both AUC values that increased and decay rates that decreased in a sigmoidal fashion as a function of DPEPC concentration (supplemental Fig. 3).

For all instances studied, the fact that the fluorescence signal was lost more rapidly in the presence of increased anionic lipid concentration and was retained more readily with increased cationic lipid concentration clearly suggests that electrostatic interactions play an important in role in the interactions between the reporter molecule C_{11}-Bodipy 581/591 and the radical initiator AAPH. The fact that the fluorescence decay rate of C_{11}-Bodipy 581/591 correlates to its rate of oxidation by AAPH radicals (Apak et al., 2016) and that C_{11}-Bodipy 581/591 rate of oxidation was either enhanced or retarded by anionic and cationic lipids, respectively, further suggests that the rate of lipid oxidation can be enhanced or limited if anionic or cationic lipids, respectively, are present

Validation of the surface charge for each liposome series was conducted by measuring the zeta potential of each sample. Results in Fig. 5 (lower panel) show that, indeed, increasing the amount of anionic lipids within the liposomes did increase the negative surface charge, and that increasing the cationic lipid present in the liposome increased the positive surface charge. We also measured liposome diameter to determine if there was size differences as function of charged lipid present. Liposomes containing DOPG were roughly 109 to 112 nm in diameter (Fig. 5, top panel). Liposomes containing DMPG had a slightly

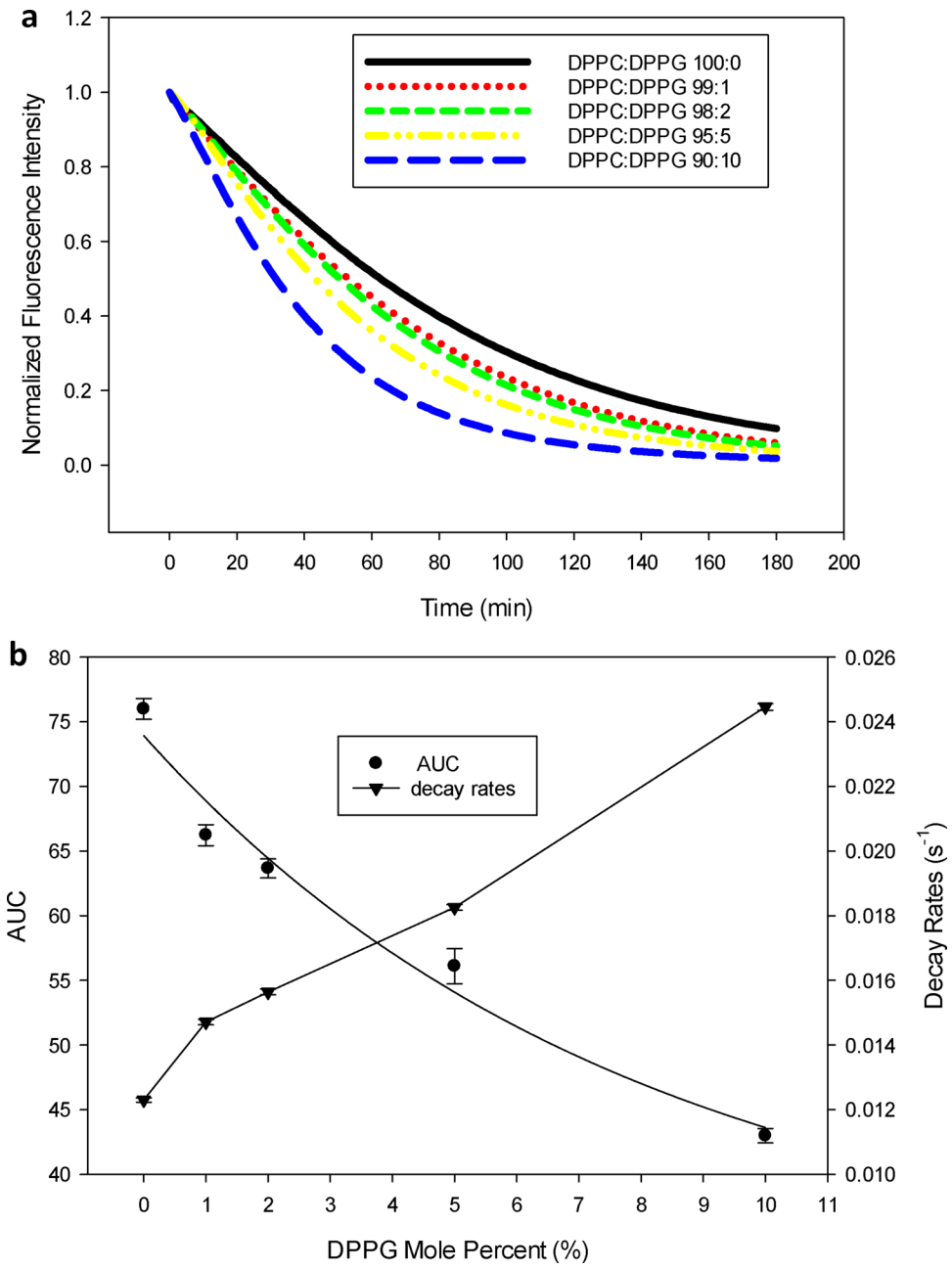

Fig. 3. a **The kinetics of the normalized fluorescence intensity for Bodipy 581/591 as a function of DPPG**. Time course for the oxidation of Bodipy 581/591 in DPPC liposome with varying concentrations of DPPG at either 0, 1, 2, 5 or 10 mol percent; oxidation was due to the thermal degradation of AAPH at 37 °C. (0, 1, 2, 5, or 10 mol percent) within DPPC liposomes. Displayed data is the average of 3–6 experiments. b **Area-under-the-curve and decay rate plot as a function of DPPG.** Values for the area-under-the-curve (left) and decay rates for the normalized fluorescence signal of Bodipy 581/591 plotted as a function of DPPG mole percent presence in DPPC liposomes. The error bars shown are the calculated standard deviations.

wider size range, from 109 to 118 nm. Both set of liposomes containing DOPG and DMPG exhibit no distinct size trend as a function of anionic lipids. Liposomes containing DOEPC, DMEPC and DPPG decreased in size as their respective concentrations increased. Liposomes containing DOEPC were roughly 112 nm with 0 mol%DOEPC present but were roughly 105 nm in diameter at 2 and 5 mol% and about 101 nm in diameter at 10 mol%DOEPC. Liposomes containing DMEPC were about 125 nm in diameter at 0 mol% DMEPC, ˜95 nm at 1 mol%, 104 to 101 nm in diameter at 2 and 5 mol%, respectively, and 107 nm at 10 mol%. Liposomes with

DPPG initially were ˜210 nm in diameter at 0 mol%, ˜168 nm at 1 mol% and finally around 155 nm at DPPG concentration above 1 mol % DOPG. Liposomes containing DPEPC exhibited the greatest size fluctuation in that they alternated between 210 and 170 nm in size (Fig. 5, top panel) over the entire mol% range explored. It would appear possible that size may affect the oxidation rate in the assay as smaller liposomes have greater curvature, which translates into tighter lipid packing and subsequently more defects that allow increased access inside the lipid membrane (Talbot et al., 1997). DOPC liposomes, however, extruded at sizes ranging from 30 to 200 nm (64 to 164 nm actual diameter) exhibited little to no difference in decay rates of fluorescence signal as data overlay one another without distinction (supplemental Fig. 4).

Apak et al., 2016 describe antioxidant activity measuring assays like the one employed herein as occurring through the transfer of a hydrogen atom transfer (Apak et al., 2016). Typically, this hydrogen atom transfer occurs between radicals generated by AAPH thermal decomposition and an antioxidant which would compete with the fluorescent probe (Bodipy 581/591). The experiments herein were minus any antioxidant. Therefore, there was no competitive kinetics occurring; instead, the AAPH radicals have direct access to the fluorescent probe for completing the one-electron oxidation. The current work shows that the

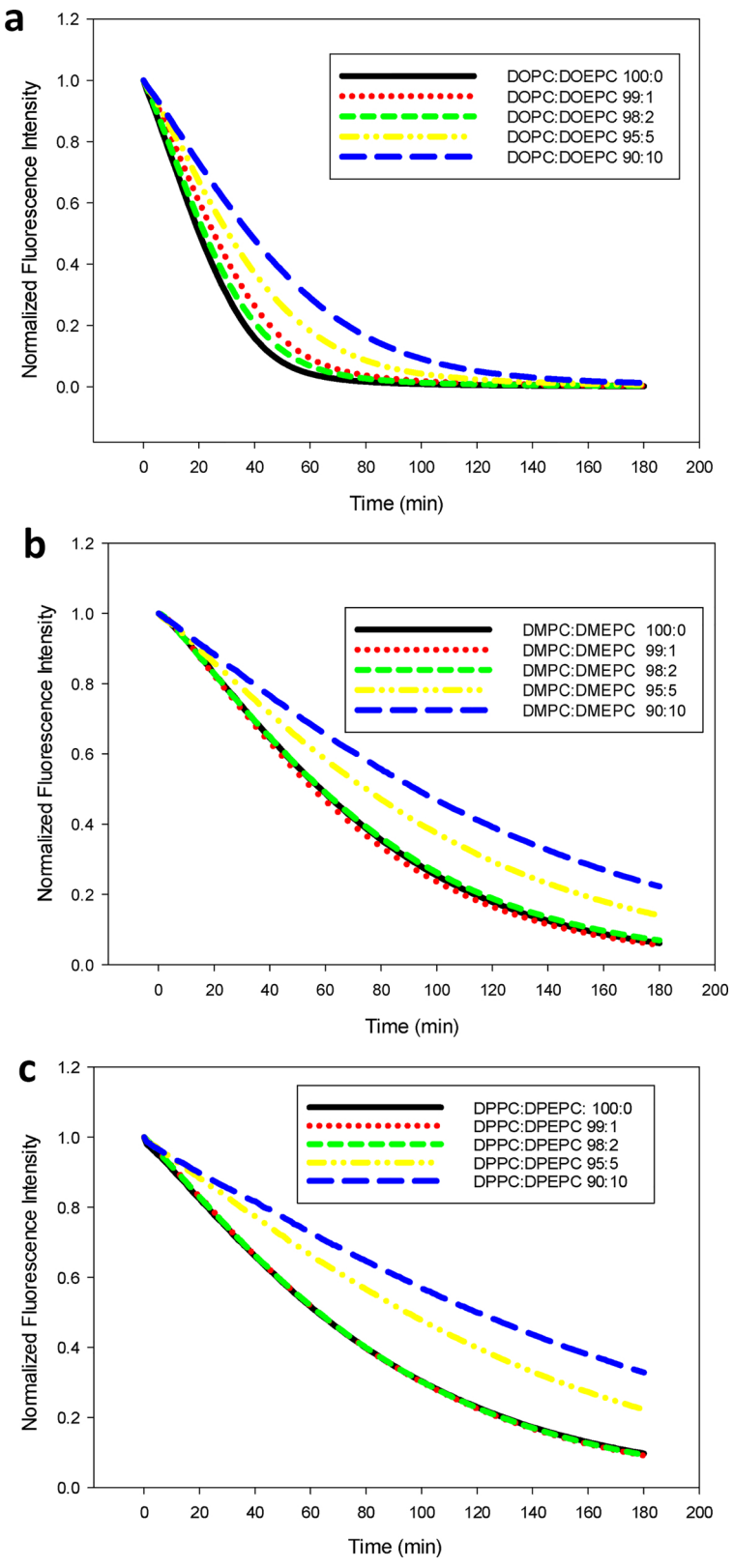

Fig. 4. a **The kinetics of the normalized fluorescence intensity for Bodipy 581/591 as a function of DOEPC**. Time course for the oxidation of Bodipy 581/591 in DOPC liposome containing varying concentrations of DOEPG at either 0, 1, 2, 5 or 10 mol percent; oxidation was due to the thermal degradation of AAPH at 37 °C. Data displayed is the average of 3–6 experiments. b **Kinetics of Bodipy 581/591 normalized fluorescence intensity as a function of DMEPC in DMPC liposomes.** Time course for the oxidation of Bodipy 581/591 as a function of DMEPC (0, 1, 2, 5, or 10 mol percent) within DMPC liposomes is displayed; oxidation was due to the thermal degradation of AAPH at 37 °C. Data displayed is the average of 3–6 experiments. c **Kinetics of Bodipy 581/591 normalized fluorescence intensity as a function of DPEPC in DPPC liposomes.** Time course for the oxidation of Bodipy 581/591 as a function of DPEPC (0, 1, 2, 5, or 10 mol percent) within DPPC liposomes is displayed; oxidation was due to the thermal degradation of AAPH at 37 °C. Data displayed is the average of 3–6 experiments.

oxidation of the fluorescent probe occurred faster in the presence of negatively charged lipids and slower in the presence of positively charged lipids. This may be due to electrostatic interactions where the AAPH radicals are more positively charged and are attracted greater to an increasingly negatively charged surface (thus a faster rate of oxidation) or are repelled greater by an increasingly positively charged surface (thus a slower rate of oxidation). There is also the possibility that the negatively charged lipids create an environment within the lipid bilayer where the fluorescent probe is an energy state where it is more easily oxidized and the positively charged lipids create an environment where the opposite is true. It is unclear, however, which is more likely.

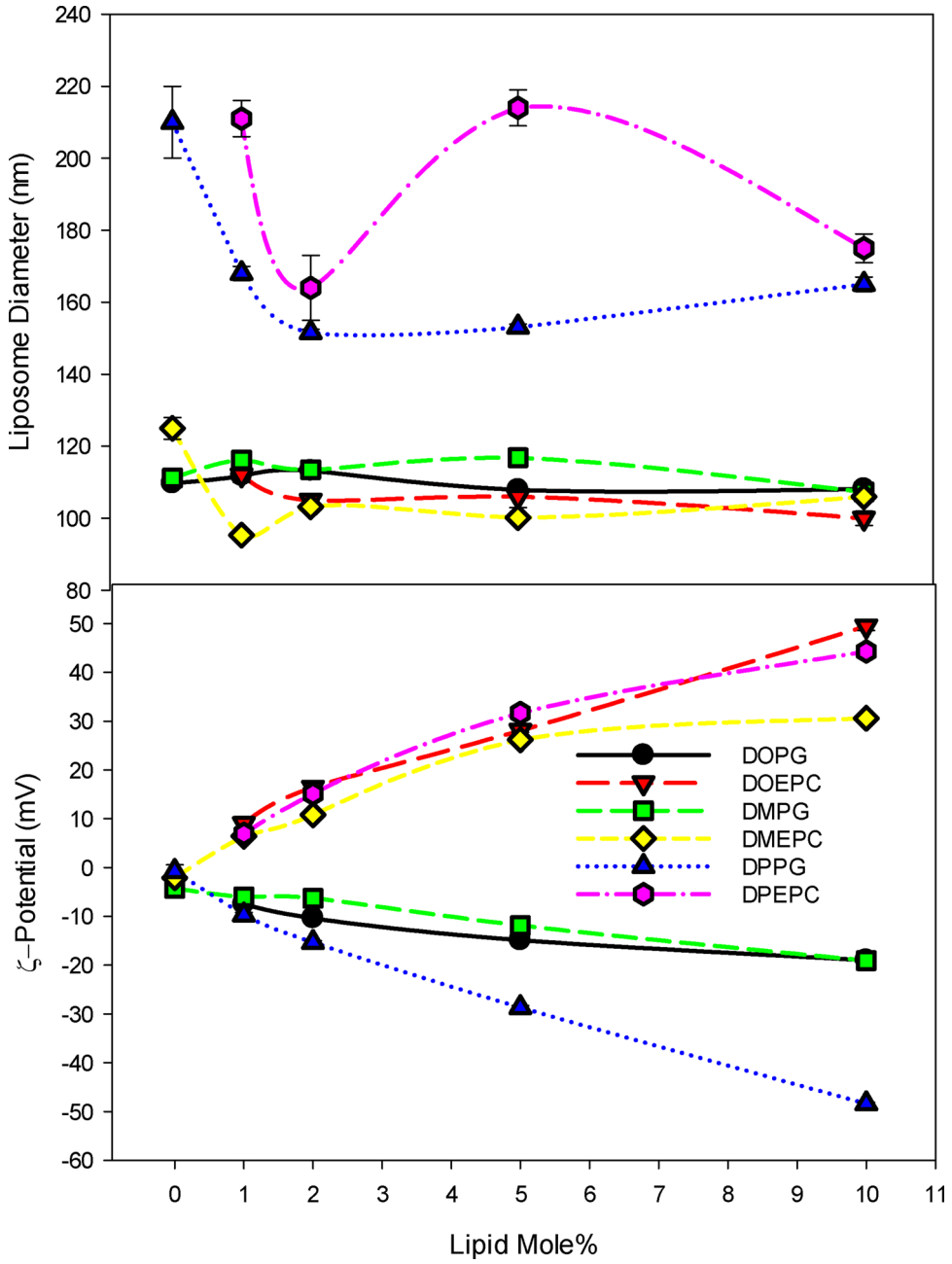

Fig. 5. Liposome diameter and ζ-potential as a function of charged lipid. The average liposome diameter (top panel) and zeta potential (bottom panel) as a function of charged lipid concentration within liposomes are displayed. The base phospholipid in liposome for DOPG and DOEPC was DOPC, for DMPG and DMEPC was DMPC, and for DPPG and DPEPC was DPPC. Error bars are ± 1 standard deviation (n = 10).

Further analysis of the decay rates for loss in fluorescence (Fig. 6) reveals that DOPG lipids induced a decay rate that was an order of magnitude faster than that induced by DMPG or DPPG, and that DOEPC lipids had decay rates that were 3 or 4 times faster than DMEPC or DPEPC lipids. These were not surprising results as lipid oxidation is fundamentally expected to proceed more rapidly in unsaturated lipids than saturated lipids. Unsaturated lipids possess one or more alkene functional groups that increase potential sites for oxidative transformations. What was surprising was that the physical state of the lipids had little or no effect on decay rates. Liposomes containing the anionic lipids DMPG or DPPG (which were in a fluid and gel state, respectively) had nearly the same decay rates and so did liposomes containing the cationic counterpart DMEPC or DPEPC (again, fluid state and gel state, respectively). This suggests that the physical state of the lipids (fluid or gel state) matters little when all lipids are saturated. This is different from the findings of Bricarello et al., 2012 who showed that the gel state of lipids further impeded fluorescence decay in liposomes (Bricarello et al., 2012). It should be noted that the lipids Bricarello et al, 2012 employed have a larger difference in phase temperatures (-1 °C/41 °C) than the lipid systems examined herein. The lipids respective phase transition temperatures can be explained by the difference in acyl chain lengths (12-carbons versus 16-carbons, respectively), whereas the ones employed in this study have phase temperature of 23 °C and 41 °C due to their respective acyl chain lengths of 14 and 16 carbons.

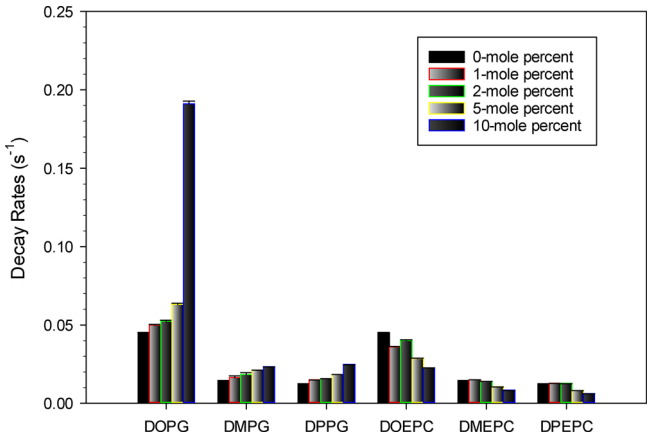

Fig. 6. Fluorescence decay rates as a function of charged lipids within liposomes. Decay rates from time course measurements of Bodipy 581/591 are display in relationship to each charged lipid investigated. Error bars are reported as the calculated standard deviation with n =. 3–6.

5. Conclusions

Various forms of the anionic lipid phosphatidylglycerol were shown to increase the oxidation of C_{11}-Bodipy 581/591 within phosphatidylcholine-based liposomes; several forms of the cationic lipid ethylphosphatidylcholine were found to retard oxidation. Saturated lipids limited enhanced oxidation induced by phosphatidylglycerol lipids but added little to the retardation ability of positively charged lipids. Overall, implications are that positively charged moieties, specifically lipids, may be used to limit oxidation of other lipids for such uses as increasing the shelf-life of edible oils, improving the useful lifetime of lubrication oils, limiting oxidation in fats used in food and beverage processes, or increasing shelf life of paints and pigments.

Conflict of interest

None.

Acknowledgements

The authors greatly appreciate and recognize the professional technical assistance provided by Ms. Leslie Smith. Mention of trade names or commercial products in this publication is solely for the purpose of providing specific information and does not imply recommendation or endorsement by the United States Department of Agriculture (USDA). USDA is an equal opportunity provider and employer.

The article was fully funded by the U.S. Department of Agriculture; thus, there were no other funders to disclose.

Appendix A. Supplementary data

Supplementary data associated with this article can be found, in the online version, at https://doi.org/10.1016/j.chemphyslip.2019.02.004.

References

An, C.-B., Li, D., Liang, R., Bu, Y.-Z., Wang, S., Zhang, E.-H., Wang, P., Ai, X.-C., Zhang, J.-P., Skibsted, L.H., 2011. Chain length effects in isoflavonoid daidzein alkoxy derivatives as antioxidants: a quantum mechanical approach. J. Agric. Food Chem. 59 (23), 12652–12657.

Apak, R., Özyürek, M., Güçlü, K., Çapanoğlu, E., 2016. Antioxidant Activity/Capacity measurement. 2. Hydrogen atom transfer (HAT)-based, mixed-Mode (electron transfer (ET)/HAT), and lipid peroxidation assays. J. Agric. Food. Chem. 64 (5), 1028–1045.

Balanč, B.D., Ota, A., Djordjević, V.B., Šentjurc, M., Nedović, V.A., Bugarski, B.M., Ulrih, N.P., 2015. Resveratrol-loaded liposomes: interaction of resveratrol with phospholipids. Eur. J. Lipid Sci. Technol. 117 (10), 1615–1626.

Bricarello, D.A., Prada, M.J., Nitin, N., 2012. Physical and chemical modifications of lipid structures to inhibit permeation of free radicals in a supported lipid membrane model. Soft Matter 8 (43), 11144–11151.

Compton, D.L., Goodell, J.R., Berhow, M.A., Kenar, J.A., Cermak, S.C., Evans, K.O., 2017. Feruloylated products from coconut oil and shea butter. JAOCS J. Am. Oil Chem. Soc. 94 (3), 397–411.

Evans, K.O., 2006. Room-temperature ionic liquid cations act as short-chain surfactants and disintegrate a phospholipid bilayer. Colloids Surf. A 274 (1-3), 11–17.

Evans, K.O., Compton, D.L., 2017. Phosphatidyl-hydroxytyrosol and phosphatidyl-tyrosol bilayer properties. Chem. Phys. Lipids 202, 69–76.

Laszlo, J.A., Evans, K.O., Vermillion, K.E., Appell, M., 2010. Feruloyl dioleoylglycerol antioxidant capacity in phospholipid vesicles. J. Agric. Food. Chem. 58 (9), 5842–5850.

Laszlo, J.A., Cermak, S.C., Evans, K.O., Compton, D.L., Evangelista, R., Berhow, M.A., 2013. Medium-chain alkyl esters of tyrosol and hydroxytyrosol antioxidants by cuphea oil transesterification. Eur. J. Lipid Sci. Technol. 115, 363–371.

Mei, L., McClements, D.J., Wu, J., Decker, E.A., 1998. Iron-catalyzed lipid oxidation in emulsions as affected by surfactant, pH and NaCl. Food Chem. 61 (3), 307–312.

Mei, L., McClements, D.J., Decker, E.A., 1999. Lipid oxidation in emulsions as affected by charge status of antioxidants and emulsion droplets. J. Agric. Food Chem. 47 (6), 2267–2273.

Mosca, M., Ceglie, A., Ambrosone, L., 2011. Effect of membrane composition on lipid oxidation in liposomes. Chem. Phys. Lipids 164 (2), 158–165.

Talbot, W.A., Zheng, L.X., Lentz, B.R., 1997. Acyl chain unsaturation and vesicle curvature alter outer leaflet packing and promote poly(ethylene glycol)-mediated membrane fusion. Biochemistry 36 (19), 5827–5836.

Tikekar, R.V., Nitin, N., 2011. Effect of physical state (solid vs. Liquid) of lipid core on the rate of transport of oxygen and free radicals in solid lipid nanoparticles and emulsion. Soft Matter 7 (18), 8149–8157.

Yoshida, Y., Niki, E., 1992. Oxidation of methyl linoleate in aqueous dispersions induced by copper and iron. Arch. Biochem. Biophys. 295 (1), 107–114.

Zhang, J., Stanley, R.A., Melton, L.D., 2006. Lipid peroxidation inhibition capacity assay for antioxidants based on liposomal membranes. Mol. Nutr. Food Res. 50 (8).